Weather and Climate Extremes 33 (2021) 100363

Contents lists available at ScienceDirect

Weather and Climate Extremes

journal homepage: www.elsevier.com/locate/wace

Extreme wind projections over Europe from the Euro-CORDEX regional climate models

Stephen Outten [a,*], Stefan Sobolowski [b]

[a] Nansen Environmental and Remote Sensing Center, Bjerknes Centre for Climate Research, Bergen, Norway
[b] NORCE Norwegian Research Centre, Bjerknes Centre for Climate Research, Bergen, Norway

ARTICLE INFO

Keywords:
Extreme wind
Extreme value analysis
CORDEX
EuroCORDEX
Future projections
Regional climate modelling

ABSTRACT

Extreme weather events represent one of the most visible and immediate hazards to society. Many of these types of phenomena are projected to increase in intensity, duration or frequency as the climate warms. Of these extreme winds are among the most damaging historically over Europe yet assessments of their future changes remain fraught with uncertainty. This uncertainty arises due to both the rare nature of extreme wind events and the fact that most model are unable to faithfully represent them. Here we take advantage of a 15 member ensemble of high resolution Euro-CORDEX simulations (~12 km) and investigate projected changes in extreme winds using a peaks-over-threshold approach. Additionally we show that – despite lingering model deficiencies and inadequate observational coverage – there is clear added value of the higher resolution simulations over coarser resolution counterparts. Further, the spatial heterogeneity and highly localised nature is well captured. Effects such as orographic interactions, drag due to urban areas, and even individual storm tracks over the oceans are clearly visible. As such future changes also exhibit strong spatial heterogeneity. These results emphasise the need for careful case-by-case treatment of extreme wind analysis, especially when done in a climate adaptation or decision making context. However, for more general assessments the picture is more clear with increases in the return period (i.e. more frequent) extreme episodes projected for Northern, Central and Southern Europe throughout the 21st century. While models continue to improve in their representation of extreme winds, improved observational coverage is desperately needed to obtain more robust assessments of extreme winds over Europe and elsewhere.

1. Introduction

The world has steadily warmed over the last 50 years, with most of the observed warming *very likely* caused by the anthropogenic emission of green house gasses (Myhre et al., 2013). The rise in global temperatures and associated impacts represent one of the greatest threats facing mankind. In particular, changes in the magnitude and frequency of extreme events are among the most concerning of these (Beniston et al., 2007; Forzieri et al., 2016). Since the start of the 21st century, Europe has experienced numerous catastrophic extreme events, including the heat waves of 2003 and 2010 (Beniston, 2004; Robine et al., 2008; Grumm, 2011), which together resulted in over one hundred thousand fatalities (MunichRE, 2020); the vast floods of 2002 and 2013 (Ulbrich et al., 2003; Grams et al., 2014), which caused over twenty-five billion euros in combined damage (MunichRE, 2020); and the cold wave of 2005–2006 (Scaife and Knight, 2008), which brought some of the coldest winter temperatures to Europe in recent decades and nearly a billion euros in crop damages.

Despite the losses caused by these types of extreme events, it is extreme winds that regularly cause the largest economic damage to Europe. The international reinsurance group, MunichRe, estimates that approximately 60% of insured losses during the period of 2000–2018 were due to meteorological events, primarily extreme winds (MunichRe, 2011; MunichRE, 2020). Apart from the insurance industry, other business sectors also rely on knowledge of extreme winds. Safe design and construction of large buildings and infrastructure depend upon accurate estimates of extreme winds. Such estimates are also important for afforestation since physiological and mechanical effects of intense winds control growth and survival of newly planted trees (Quine, 2013). Wind power is another sector that relies upon good knowledge of extremes winds, both to avoid damage to wind turbines, but also to minimise cut-out, where the turbines stop producing electricity if the wind speed is too high. Given the growing needs of these industries, and the damage and loss of life extreme winds can cause, robust and reliable assessments of the frequency and intensity of extreme wind events are of growing importance for society.

* Corresponding author.
E-mail address: stephen.outten@nersc.no (S. Outten).

https://doi.org/10.1016/j.wace.2021.100363
Received 10 December 2020; Received in revised form 6 May 2021; Accepted 29 July 2021
Available online 7 August 2021

Previous studies have examined the climatology of extreme winds in reanalyses. Della-Marta et al. (2009) examined extreme winds in the ERA40 reanalysis produced by the European Centre for Medium-Range Weather Forecasts (ECMWF). They used the 10-metre wind speed and wind gusts in their analysis. However. wind gusts in ERA-40 are derived from a parameterisation and are unrealistic, especially in coastal regions and close to topography. One issue with examining winds directly in reanalysis is that, since turbulent energy cascades from larger scales to smaller scales, extreme winds are a local-scale effect. This means that in order to capture extreme winds, a high horizontal resolution is required. When a lower resolution is used, any intense wind that might occur is effectively averaged out over the grid box, thereby producing lower wind speeds. The ERA40 reanalysis examined by Della-Marta et al. (2009) has a resolution of only 1.125°, equivalent to a grid spacing approximately 125 km, which is unsuitable for capturing extreme winds over complex terrain.

Some studies have used an alternative approach to utilising the wind speeds directly. Instead, they determine the geostrophic wind speed based on the mean sea level pressure. Donat et al. (2016) examined both wind speeds and MSLP in ERA40, the NOAA 20th century and the NCEP reanalyses, however these reanalyses all have relatively coarse resolutions. While this allowed Donat et al. (2016) to determine broad trends in storminess over large regions, it was insufficient for identifying fine details of extreme winds over Europe. A similar approach was also used by Wang et al. (2011) but for observations from twenty meteorological stations, and similar trends in storminess were determined for large regions.

The second major problem that underlies many extreme wind studies that use reanalysis and observations stems from the temporal sampling of winds. The 10-metre wind speed or MSLP used in these studies are instantaneous values output at six hour intervals. Some stations in the Wang et al. (2011) study provided outputs at three hourly intervals, as do the newer generation of reanalyses. Since it is highly unlikely that the peak winds will occur at the instant of sampling, this approach ensures that the highest wind speeds are missed and hence the extreme winds are underestimated. Taking six-hourly samples of ten-minute winds results in an underestimation of the extreme events by approximately 15% (Larsen and Mann, 2006).

More recent studies have focused on the assessment of extreme winds in regional climate models (RCMs). These are used to dynamically downscale both reanalyses and climate models to much higher spatial resolutions. Since RCMs are also used to downscale climate models, they can provide some insight into future changes of extreme winds by downscaling both historical and future projections from the climate models. One issue with RCMs is that they have been shown to underestimate wind speeds when compared to observations (Kunz et al., 2010), however as the horizontal resolution of RCMs has increased, this gap has narrowed (Hewson and Neu, 2015).

Early studies examined the regional simulations produced by the Prediction of Regional Scenarios and Uncertainties for Defining European Climate Change Risks and Effects (PRUDENCE, EU FP5 project) project (Beniston et al., 2007; Rockel and Woth, 2007; Schwierz et al., 2010). The simulations in PRUDENCE had a horizontal resolution of 50 km. These studies examined the change between an historical period of 1961–1990 and a future period of 2071–2100. To identify extreme winds, they looked at the 95th, 98th, and 99th percentiles of 10-metre wind speed. All three studies showed a projected increase in winds speeds over Northern Europe with decreased wind speeds over the Mediterranean between the two periods.

Subsequent studies examined the output from the successor to PRUDENCE, the Ensemble-Based Predictions of Climate Changes and their Impacts (ENSEMBLES, EU FP6 project) project (Donat et al., 2011; Pryor et al., 2012; Outten and Esau, 2013). The ENSEMBLES simulations were produced with a horizontal grid spacing of 25 km, allowing for the first time some of the details of extreme wind spatial distributions to be identified. Also, the RCMs in ENSEMBLES output the maximum daily wind speed. This is the highest wind speed that occurs during any time step of the day, hence greatly reducing the sampling problem. Donat et al. (2011) examined the 98th percentile of wind speeds, while Pryor et al. (2012) and Outten and Esau (2013) both examined the 50-year return levels of wind. All three showed a projected increase in wind speed over Northern Europe, with Donat et al. (2011) and Outten and Esau (2013) showing a projected decrease in extreme winds over the Mediterranean. In all cases, the largest changes were found over the ocean, with changes over land being classified as 'spotty' or non-consistent between individual simulations, similar to the findings of other studies (e.g. Nikulin et al., 2011). It should be noted that Donat et al. (2011) examined fourteen simulations from the ENSEMBLES project, while Pryor et al. (2012) and Outten and Esau (2013) examined two and four respectively. One reason for the smaller number of simulations examined in the Pryor et al. (2012) and Outten and Esau (2013) studies was the computational demand of performing extreme value analysis to derive the 50-year return levels.

As is clear from the studies discussed here, extreme winds are assessed in a variety of ways. Reviews of the different methodologies are given in Palutikof et al. (1999) and Perrin et al. (2006). The simplest approach is to examine a high percentile of the wind speeds available in the data, for example, the 99th percentile. However this is limited to only the data included in the data set and does not lend itself to extrapolation. More common when assessing extreme events is to fit a statistical distribution to the data, which accounts for the non-linear nature of wind speeds. A commonly used approached is the so-called Weibull method, where a Weibull distribution is fitted to the wind speeds (e.g. Quine, 2013; Lun and Lam, 2000; Koh et al., 2011). As well as assuming the wind speeds are distributed according to a Weibull distribution, this approach fits the distribution to all of the data. Thus, the upper tail of the distribution which describes the extremes, is based on the fit to the bulk of the data, which is not extreme.

Fortunately, there is a branch of mathematics called Extreme Value Analysis (EVA) that deals with extreme distributions and determining the probability of an event occurring that is more extreme than any previously observed. EVA has gained increasing use in climate science over the past decade. EVA includes two basic approaches for determining extremes. The first is the block maxima method. This is based on the Fisher–Tippett theorem that states that the maxima of multiple samples (blocks) of independent, identically distributed data will converge to one of three classic distributions: the Gumbel, the Fréchet, or the Weibull distribution (Fisher and Tippett, 1928; Gumbel, 1958). These three distribution can all be described by the single Generalised Extreme Value (GEV) distribution. The main weakness of the block maxima approach is that only the maximum value in each block is included in the analysis. This wastes a large amount of data, results in small samples and ignores multiple extreme events occurring within a single block.

The second approach in EVA is based on the Pickands–Balkema–de Haan theorem which states that the distribution of exceedances over a suitably chosen threshold will converge to a Generalised Pareto Distribution (GPD; Balkema and de Hann, 1974; Pickands, 1975). This is often called the peaks over threshold (POT) approach, and has the advantage of extracting a greater number of extreme events than the block maxima method, thus reducing the sample uncertainty by increasing the sample size. The POT has the disadvantage that the threshold needs to be carefully selected, a requirement that the GEV method does not have. A more complete review of EVA methods is given in Coles (2001).

In this study, we apply the POT approach to determine different return levels of extreme wind events, based on the daily maximum wind speed from and ensemble of fifteen Euro-CORDEX simulations, which have a grid spacing of ~12 km. We examine the details of the spatial distribution of extremes winds made possible by this high horizontal resolution, demonstrate the improvements over the lower resolution simulations of Euro-CORDEX, and investigate the future

changes projected by different GCM-RCM combinations for three future periods. The data and methods used are presented in Sections 2 and 3 respectively, with results for the historical and future periods given in Sections 4 and 5. A discussion and conclusion is given in Section 6.

2. Source data

The data examined in this work comes from the ensemble of simulations created for the European domain as part of the Coordinated Regional Downscaling Experiment (Euro-CORDEX), a major project of the World Climate Research Programme (WCRP). The CORDEX project protocol defined thirteen additional domains covering all land areas of the world (Giorgi and Gutowski, 2015). The Euro-CORDEX protocol required participating institutes to employ their respective Regional Climate Models (RCMs) to each downscale output from one or more global climate models (GCMs) of the Fifth Phase of the Coupled Model Intercomparison Project (CMIP5; Jacob et al., 2020). The CMIP5 experiments chosen for downscaling were the Historical and three projections forced by different Representative Concentration Pathway scenarios (RCP2.6, RCP4.5, and RCP8.5; van Vuuren et al., 2011). This approach produced multiple downscaled simulations of each available GCM with different RCMs for each of the scenario experiments. Despite the spareness of the RCM-GCM matrix this allows for great intercomparison of the roles and impacts of the different GCMs and RCMs on shaping the simulated regional climate. However, due to limitations in resources and data availability, not all GCMs were downscaled with all RCMs.

Here we examine fifteen of the simulations from the Euro-CORDEX ensemble, the branch of CORDEX focused on the European domain. These were chosen based on the availability of completed simulations with the required variables for both the Historical and RCP8.5 scenario experiments. The simulations examined in this study are listed in Table 1. They are all on a common domain covering Europe with a horizontal resolution of 0.11°(approximately 12.5 km). Four 30-year time-slices were selected for analysis, one from the end of the Historical experiment (1976–2005) and three from the future scenario experiments covering the near future (2011–2040), mid-century (2041–2070), and far future (2071–2100). Hereafter, these are referred to as the Historical, Near, Mid, and Far periods respectively. The time-slice length of 30 years was selected as a compromise between being long enough to provide sufficient data to produce acceptable estimates of return events and being short enough as to satisfy the identical distribution criteria required to apply EVA. This choice of time-slice length also maximises comparability with those studies because it has been commonly used in many previous works Beniston et al. (e.g. 2007), Outten and Esau (e.g. 2013), Schwierz et al. (e.g. 2010). Since the focus of the work in on extreme winds, the variable analysed is the daily maximum 10 metre wind speed.

3. Methods

The peaks over threshold (POT) method was selected for determining the return levels of extreme events in this study. The POT approach fits a Generalised Pareto Distribution (GPD) to the exceedances over a suitably chosen threshold. If the threshold is too low, the exceedances produced cannot be considered extreme and the GPD is not suitable for fitting. This results in biases being introduced (Van de Vyver and Delcloo, 2011). However, if the threshold is too high, very few exceedences are produced leading to increased variance in the parameter estimation. A commonly used approach to determine a suitable threshold is to use a plot of sample mean excess (SME). However, the threshold must be estimated from the SME plot by eye, which is a significant shortcoming. Repeating this procedure for each grid point in a single model domain is impractical, and there is no widely accepted methodology for automating the procedure for identifying thresholds. In this study, we utilise a simple approach previously employed in Outten and Esau (2013). The threshold for each grid point is selected as the lowest annual maxima wind speed in that grid point. This guarantees a minimum of 30 exceedances for 30 years of data. In practice, this approach resulted in approximately 40 to 500 exceedances for the Historical period, depending upon grid point and model. This means the exceedances were the top 0.3% to 3.6% of the wind speeds at any given grid point, with the mean percentage of exceedances across the grid points being less than 0.98% in every model. While this method does not guarantee that a threshold is suitably chosen at every grid point, it does hold for the majority of the domain. Some of the isolated locations where this method breaks down are visible in the maps of return levels as isolated grid points exhibiting either very high or very low wind speeds.

After selecting the exceedances, a simple declustering method was applied to ensure the independence of the extremes. This is a requirement for many statistical methods, including the POT method, and when combined with the identically distributed requirement discussed earlier, it is often referred to as the independent identically distributed (i.i.d.) criteria. The declustering method isolates the highest peak from any others occurring within two days on either side of the maximum, thus ensuring that each extreme is isolated from any other by at least 48 h. On rare occasions, it was found that two peaks could occur within 48 h of one another with exactly the same wind speed, most likely due to some rounding of values occurring during the production, post-processing, or analysis of these data. In these rare cases, the declustering method was found to ignore both points since neither was greater than the other. To resolve this, small random fluctuations of magnitudes up to 0.0001 ms^{-1} were added to the peaks. The largest peak was then retained and the fluctuations were subtracted to restore the original wind speed. Finally, a maximum likelihood estimation method was used to fit a GPD to the resulting exceedances. The cumulative distribution function for the GPD is given by:

$$H(y) = \begin{cases} 1 - (1 + \frac{\xi y}{\sigma})^{\frac{-1}{\xi}} & \text{for } \xi \neq 0 \\ 0 & \text{for } \xi = 0 \end{cases} \quad (1)$$

where ξ is the shape parameter and σ is the scale parameter. The GPD corresponds to the exponential, ordinary Pareto, and Pareto II type distributions where $\xi = 0$, $\xi < 0$, and $\xi > 0$ respectively. For a suitably chosen threshold, the number of exceedances can be assumed to approximate a Poisson distribution with parameter λ.

From the fitted GPD, the T year return event, U_T, is an event (or quantile) which on average is only exceeded once every T years, but more precisely is the wind that occurs in each single year with a probability of $\frac{1}{T}$ adjusted for the number of exceedances occurring each year, as given by λ. The T year return event can be calculated from

$$U_T = \begin{cases} u + \frac{\sigma}{\xi}\left[(\lambda T)^{\xi} - 1\right] & \text{for } \xi \neq 0 \\ u + \sigma ln(\lambda T) & \text{for } \xi = 0 \end{cases} \quad (2)$$

In this work, return wind speeds were determined for periods of 2, 5, 10, 20, 30, 50, 70, and 100 years. While these various return wind speeds will be used when discussing future changes, much of the following results focus on the 30-year return level of wind speeds. The 30-year return level is selected here as it provides a good example of an extreme event without being so rare as to be too far into the tail of the distribution. It also provides good comparability with other studies that have also used 30-year return level. Where uncertainties in the derived return winds are given, they are estimated using a profile likelihood approach, although a bootstrapping approach was also tested using 1000-member ensemble create with random re-sampling.

4. Extreme winds in Euro-CORDEX

We start the assessment of extreme winds at a single grid point in a single simulation in our Historical period. Here we have selected the grid point closest to the city of Bergen, Norway, in the RCA4

Table 1
List of Euro-CORDEX simulations used in this study, with the respective modelling centre, global climate model downscaled, regional climate model, and abbreviated simulation name.

Institution	Global model	Regional model	Short name
CLM Community - BTU Cottbus	CNRM-CM5-LR	CCLM4-8–17	CLMcom_CNRM
CLM Community - BTU Cottbus	EC-EARTH	CCLM4-8–17	CLMcom_ICHEC
CLM Community - ETH Zurich	HadGEM2-ES	CCLM4-8–17	CLMcom_MOHC
CLM Community - BTU Cottbus	MPI-ESM-LR	CCLM4-8–17	CLMcom_MPI
Danish Meteorological Institute	HadGEM2-ES	HIRHAM5v1	DMI_MOHC
Danish Meteorological Institute	NorESM1-M	HIRHAM5v2	DMI_NorESM
Laboratoire des Sciences du Climat et de l'Environnement	IPSL-CM5A-MR	WRF331F	IPSL_IPSL
Royal Netherlands Meteorological Institute	EC-EARTH	RACMO22E	KNMI_ICHEC
Royal Netherlands Meteorological Institute	HadGEM2-ES	RACMO22E	KNMI_MOHC
Max Plank Institute	MPI-ESM-LR	REMO2009	MPI_MPI
Swedish Meteorological and Hydrological Institute	CNRM-CM5-LR	RCA4	SMHI_CNRM
Swedish Meteorological and Hydrological Institute	EC-EARTH	RCA4	SMHI_ICHEC
Swedish Meteorological and Hydrological Institute	IPSL-CM5A-MR	RCA4	SMHI_IPSL
Swedish Meteorological and Hydrological Institute	HadGEM2-ES	RCA4	SMHI_MOHC
Swedish Meteorological and Hydrological Institute	MPI-ESM-LR	RCA4	SMHI_MPI

simulation driven by the EC-Earth model (SMHI_ICHEC). The curve of the GPD is fitted to the exceedances over the threshold and the return wind speeds at various levels are found (Fig. 1). In this model, the 10-year and 100-year return events are 20.8 ms^{-1} and 22.3 ms^{-1} respectively, a difference of only 1.5 ms^{-1}. The confidence interval on these return winds are 20.1 to 22.1 ms^{-1} and 21.2 to 25.3 ms^{-1} respectively. When we compare this fitted GPD curve to those of the fourteen other simulations for the same grid point (Fig. 1), the spread between the different simulations becomes clear. The 30-year return wind speed varies between 12.9 ms^{-1} in CCLM driven by the CNRM climate model (CLMCom_CNRM) and 28.3 ms^{-1} in HIRHAM5 driven by the Norwegian Earth System model (DMI_NorESM), with confidence intervals of 12.5 to 14.1 ms^{-1} and 26.8 to 33.0 ms^{-1} respectively. This means the inter-simulation range, i.e. from the model with the lowest value to the model with the largest value, is 15.4 ms^{-1}, or more than an order of magnitude greater than the difference between the 10-year and 100-year return level events in the SMHI_ICHEC simulation. This matches with previous findings of Outten and Esau (2013) who found that the greatest uncertainty was from the disagreement between models.

Examining the curves in Fig. 1, it is clear that there is some distinct grouping of the curves based on the RCM employed. Most apparent are the CLMcom simulations which all show far lower values than any of the others. Similarly, the DMI and IPSL simulations appear distinctly higher than any others. Removing these from consideration, the range between the remaining eight simulations reduces to 1.6 ms^{-1}. This is no indication that the remaining eight models are somehow more accurate since the choice of which models to remove for this example is subjective, however, the reason for this grouping based on RCM and the large range between the simulations for this particular grid point, becomes clear when placed in the broader context of extreme winds across Europe.

Once again we examine the single simulations of SMHI_ICHEC, still for our Historical period, but now focusing on just the 30-year return level wind speed but for all grid points in the domain (Fig. 2). The most striking feature is the land–sea contrast, with most of mainland Europe exhibiting 30-year return wind speeds of around 15 ms^{-1}, while the North Atlantic, including the North and Nordic seas, are closer to 30 ms^{-1}. The inland seas, including the Mediterranean, Black, and Baltic Seas, are relatively sheltered by the surrounding land and show 30-year return wind speeds of around 25 ms^{-1}. Thanks to the high resolution of these Euro-CORDEX simulations, far more details of the distribution of extreme winds are visible than was the case in previous generations (such as the ENSEMBLES project).

First, SMHI_ICHEC appears to have higher wind speeds around mountain ranges, such as the Scandes mountains, the Alps (especially between Italy and France), the Pyrenees between France and Spain, and the High Atlas mountains in Morocco. Even the Scottish Highlands in the U.K. exhibit a distinct peak in wind speeds. Some details of these mountain ranges are directly visible in the distribution of 30-year return wind speeds, such as the impacts of individual valleys in the Norwegian mountains that act as channels(shelters) on the windward(leeward) sides of the mountains. Second, while the lower frictional drag of the sea surface results in higher wind speeds over the sea than land, extreme winds at a given location are often the result of the passing of specific storms. In a thirty year time slice, such as our Historical period, the 30-year return level wind speed can easily be determined by the passage of a single storm. This effect is clearly visible over the North Atlantic, and even in the Mediterranean, where paths of individual, intense storms are visible as tracks of particularly high 30-year return wind speeds.

Third, the presence of cities causes increased drag on the atmosphere, reducing wind speeds, especially the extremes. While this effect is present across Europe, it is difficult to distinguish. However, due to the flatness and exposure of the U.K., the drag effect of major cities is clearly shown. Over much of the U.K., the 30-year return wind speed is around 23 ms^{-1}, but this drops to around 15 to 18 ms^{-1} in small regions over London, Manchester, Birmingham, Leeds, Sheffield, Nottingham, Newcastle, and Glasgow. Some of these cities are around the same size as a single grid point in the model domain, but their drag affects the wind speeds in surrounding grid boxes as well, making them visible.

Fig. 2 has a small number of individual grid points which appear to have anomalously high or low 30-year return wind speeds compared to the surroundings (the effect is especially clear over Finland and Northern Russia). These are locations where the chosen threshold was inappropriate and the derived extreme winds are not realistic. There is currently no widely accepted, robust method for automatically selecting a suitable threshold. However, since the GPD is fitted to each grid cell individually, the impacts of the few locations where the threshold is inappropriate are limited to individual grid cells and they have no effect on surrounding grid points or the broader picture.

By comparing similar plots of 30-year return wind speeds across Europe for all fifteen simulations, we are in a position to undertake some model intercomparison to identify the effects of both the regional and global models (Fig. 3). Each of these plots is shown individually as in Fig. 2 in the Supplementary Material.

The four CLMcom simulations all have consistently lower wind speeds over the mountain ranges compared to the others, while the five SMHI simulations all have consistently higher wind speeds over the same locations. The differences are likely due to how the different RCMs treat the effects of mountains, most likely due to differences in their roughness lengths or orographic blocking schemes over this terrain type. The grid point closest to the city of Bergen, Norway is located close to the Norwegian mountains, so this difference between the RCMs is responsible for the wide spread seen in Fig. 1. In both the SMHI and CLMcom simulations the effects of the mountains are

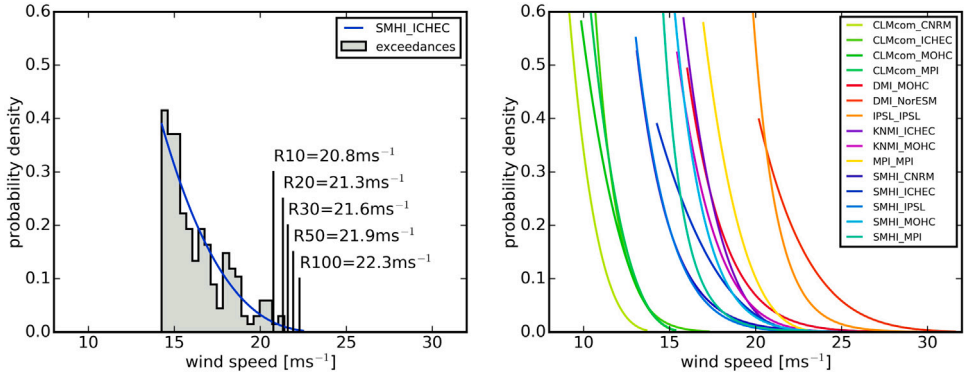

Fig. 1. Left: GPD curve (blue) fitted to exceedances (grey bars) of maximum daily wind speed for the grid point closest to the city of Bergen, Norway in SMHI_ICHEC. This is for our historical period (1976–2005). The return wind speed at the 10, 20, 30, 50, and 100 year levels are marked (black). Right: Comparison of the curves of the fitted GPDs in all fifteen downscalings.

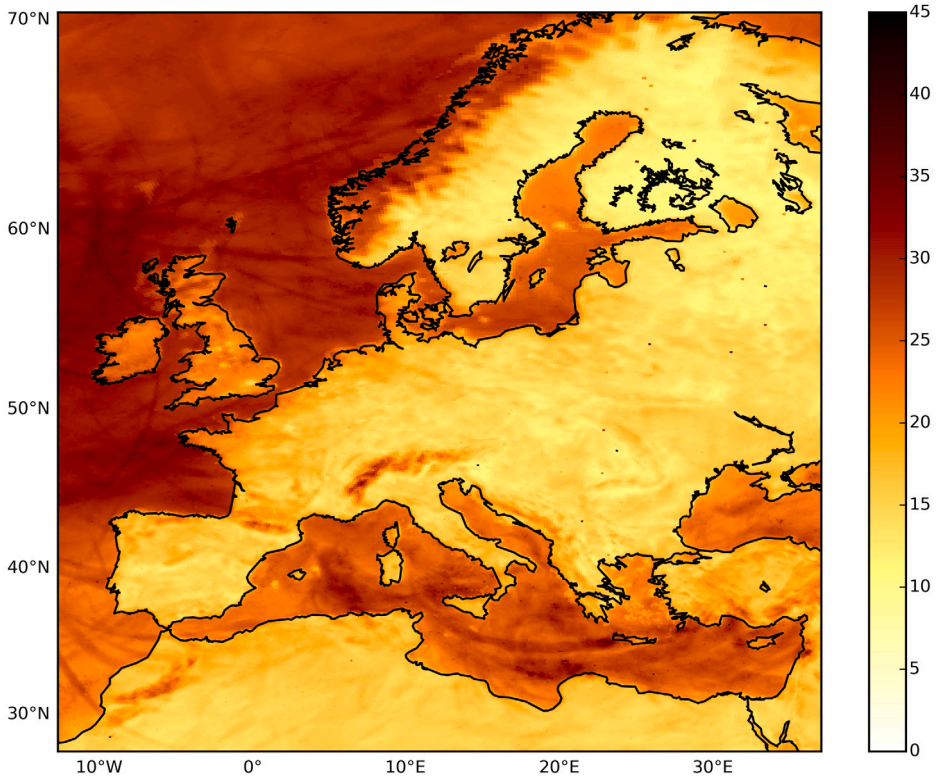

Fig. 2. 30-year return wind speed for our historical period (1976–2005) over the Euro-CORDEX domain in the SMHI_ICHEC downscaling based on GPD fitted to exceedances of daily maximum wind speed. Units are ms^{-1}.

generally only visible for the highest mountain ranges (e.g. High Atlas and not the entire Atlas mountain range). However, the effect is so much greater in the IPSL RCM, which produces much higher wind speeds around orography, that all the mountain ranges in Europe are clearly visible in the IPSL_IPSL plot in Fig. 3 (and in Figure S7 in the Supplementary material, which shows just the IPSL_IPSL plot). This leads to higher extreme winds in the IPSL simulation across most of the Alps, the numerous Sierras of Spain, the Atlas mountain chain across Morocco, Algeria and Tunisia, the Carpathian Mountains in Slovakia and Romania, the mountains of the eastern Adriatic countries, and Taurus mountains of Turkey.

A similar effect is also apparent in the DMI simulations, which appear to have a very low roughness length over water and thus much greater wind speeds over water compared to the other RCMs. There is a distinct difference in the representation of winds over mountains in the DMI downscalings of HadGEM2-ES and NorESM, most clearly visible over the Alps, due to changes between version 1 and 2 of the HIRHAM5 model respectively. Although difficult to see in detail, Fig. 3 also shows that the drag effect of cities is related to the RCM. The CLMcom simulations show lower wind speeds mostly limited to over major cities, very similar to what is seen in the SMHI simulations (e.g. Fig. 2). A very different picture is observed in the KNMI simulations, which show no visible decrease in the extreme winds over cities. This can be seen more clearly when comparing the extreme winds over the U.K only (Supplemental Figure S16).

Knowing and appreciating these differences between the RCMs is important when undertaking any study using these models. However, this becomes even more important as simulations such as these are being increasingly used in making assessments of extreme events for adaptation planning. For example, when planning large construction on the outskirts of a city, estimates of extreme winds from the KNMI model may be inappropriate to use. It may produce extreme winds estimates

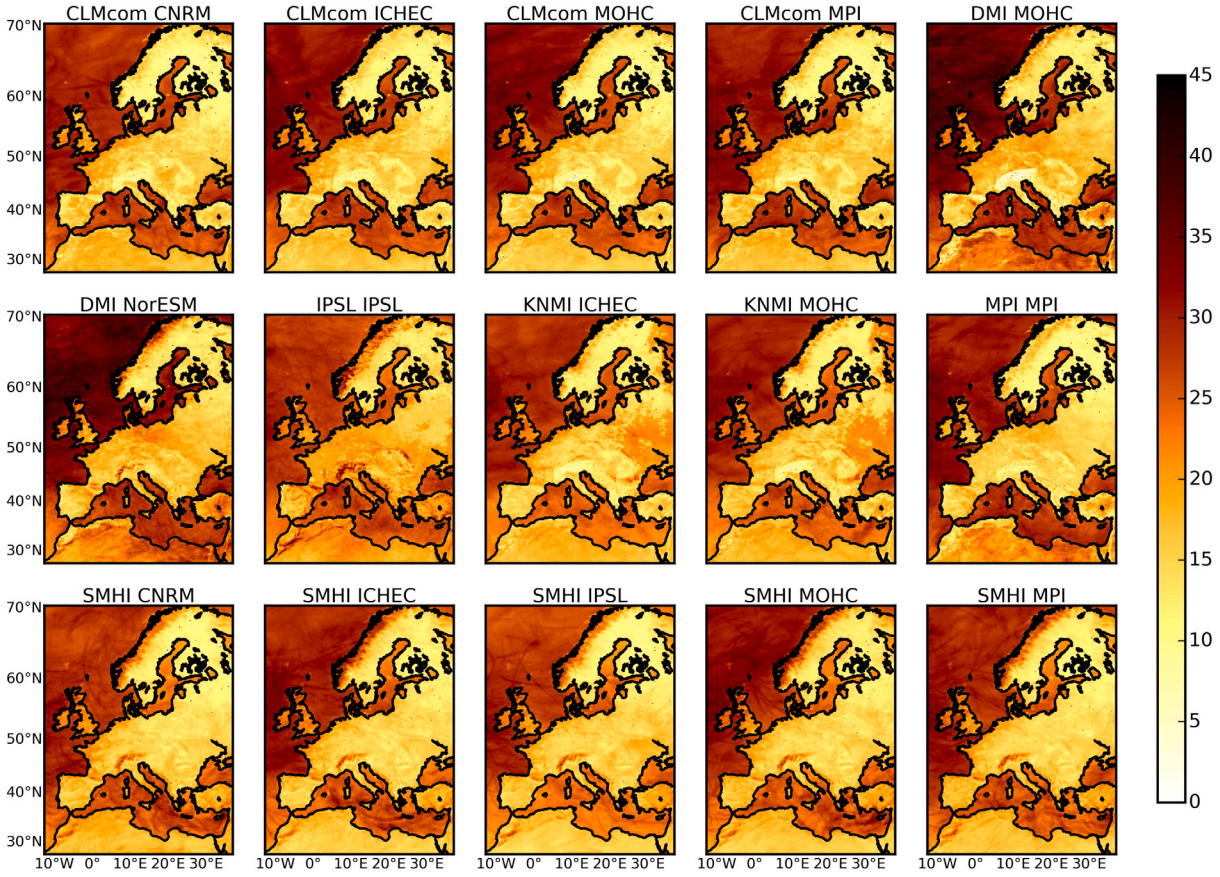

Fig. 3. 30-year return wind speed for our historical period (1976–2005) over the Euro-CORDEX domain in all fifteen simulations based on GPD fitted to exceedances of daily maximum wind speed. Units are ms^{-1}.

comparable to what is observed, but it would be doing so for the wrong reasons if the model is underestimating or completely lacking the drag caused by the city itself, as suggested by Fig. 3.

More subtle but still present are the impacts of the driving GCMs. As small scale variations in the land surface greatly impact the wind speeds, the effects of the GCMs are most clearly visible over the seas, especially the North Atlantic. For this we focus on three RCM-GCM pairs from the CLMcom, KNMI, and SMHI RCMs, where each pair downscaled the EC-EARTH and HadGEM2-ES GCMs (ICHEC and MOHC respectively). In all three pairs, the downscaling of the MOHC model shows generally higher wind speeds over the North Atlantic compared to the downscaling of the ICHEC model, due to the higher wind speeds coming from the global model. Despite being attenuated by the RCMs, the differences from the GCMs are still present over land, and may be identifiable over coastal regions, especially over the U.K. However, with so few comparisons in this fifteen member ensemble where the same GCM is downscaled by multiple RCMs, there is insufficient information upon which to base a more rigorous assessment of the impacts of the GCMs. This issue can potentially be investigated in more detail thanks to the recent growth of the Euro-CORDEX ensemble (Coppola et al., 2021; Vautard et al.).

One final feature regarding the wind speeds over the seas are the previously mentioned paths of storms, visible as tracks of higher 30-year return wind speeds in Fig. 3. There appears to be no consistency in the location or intensity of the tracks between simulations using either the same RCM or the same GCM. Intense storms will be passed from the GCM to the RCM through the boundary conditions, so this lack of consistency indicates that an intense storm entering the domain from the GCM does not necessarily result in an intense storm in the RCM. The fact that the storm tracks and intensities do not align perfectly arises in part due to the freely evolving atmosphere and large domain of the RCMs, and in part due to the smooth SSTs inherited from the coupled AOGCMs, which are uncoupled in the RCM.

Finally, we examine the importance of resolution on reproducing extreme winds. Most CORDEX simulations are run at a standard resolution of 0.44°(approximately 50 km). Euro-CORDEX simulations also targeted the higher resolution examined here of 0.11°, or approximately 12.5 km. Fig. 4 compares the 30-year return wind speed in the SMHI_ICHEC simulations at these different resolutions. The left plot is the 0.11°simulations (previously shown in Fig. 2), the right plot is the 0.44°resolution simulations and the centre plot is the high resolution simulation interpolated (upscaled) onto the 0.44°resolution horizontal grid. If the increased resolution had little impact on the extreme winds produced, the upscaled plot would be very similar to the low resolution plot. However, there are numerous striking differences.

The magnitude of the extreme winds is generally higher across the whole domain in the upscaled plot compared to the lower resolution plot. The winds are far more heterogeneous over the land, with the impacts of coastal region, mountains, cities, and other land-surface types having a much stronger influence due to the higher resolution of the underlying simulation. Mountainous regions not only show higher wind speeds and larger areas of influence, but presence and effect of individual valleys is still visible in the upscaled plot (e.g. Norwegian mountains). Perhaps most striking though are the differences over water. Over the seas, most of the finer scale structures are completely missing from the low resolution downscaling. This is especially obvious over the Mediterranean where all the structure is lost and the extreme winds are around 5 ms^{-1} lower. This plot clearly demonstrates the added value of the higher resolution simulations, and raises serious concerns for assessing extreme winds in any simulations over other CORDEX domains where only the lower resolution simulations are available.

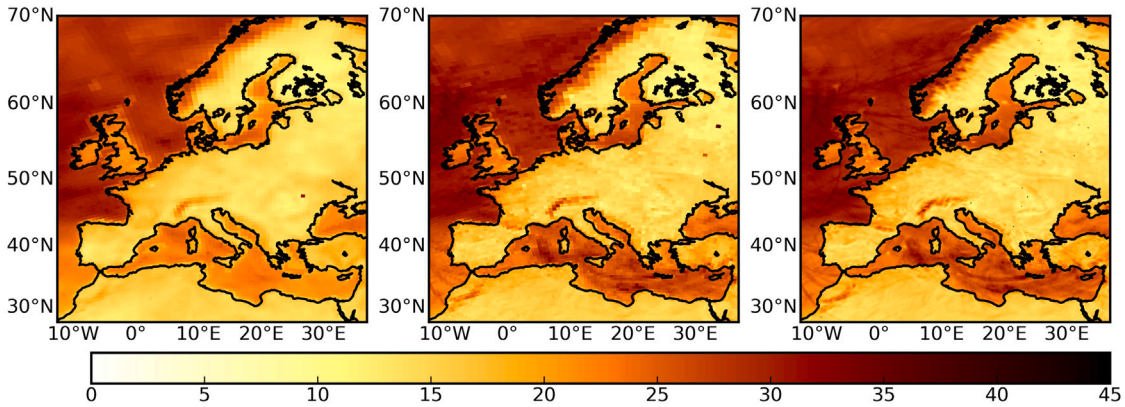

Fig. 4. Comparison of the 30-year return wind speed for our historical period in the SMHI_ICHEC downscalings on the 0.44 degree resolution (left) and the 0.11 degree resolution (right) Euro-CORDEX domains. The 0.11°resolution is also shown interpolated (upscaled) onto the 0.44°resolution grid (middle). Units are ms^{-1}.

5. Projected future changes in extreme winds

We now examine the extreme winds in the Near (2011–2040), Mid (2041–2070) and Far (2071–20100) future time slices. These are shown for all models in Supplemental Figures S17, S18, and S19 for the Near, Mid, and Far future periods respectively, in a similar format to Fig. 3.

Given the spread between the different RCMs as discussed in the previous section, and shown in Figs. 1 and 3, the Historical and Future extreme winds are first compared in an ensemble consisting of only the five SMHI simulations (bottom row of Fig. 3). The range of 30-year return wind speed between the SMHI downscalings in the Historical period is between 1 and 2 ms^{-1} over much of the land, rising to around 4 to 5 ms^{-1} in some mountainous and coastal areas (Fig. 5). The range over the sea is far greater in isolated locations. However, since the extreme winds over the seas are strongly tied to the passage of individual storms, these locations showing large ranges only serve to highlight the differences in the positions of storm tracks between the simulations.

The mean change between the Historical and Future time slices in the SMHI simulations is around ±1 ms^{-1} over much of the land, with few locations reaching ±2 ms^{-1} (e.g. the Scandes Mountains, Alps). Changes over the seas, especially over the Mediterranean, are larger, but again this is mostly a reflection of the differences in the positions of intense storms that are responsible for extreme winds. Large changes are seen over the Saharan Desert, and these consistently increase going into the future. In general though, as noted in previous studies (e.g. Outten and Esau, 2013), the future change in extreme winds is comparable or smaller than the range between the simulations in the Historical period. A similar comparison was undertaken using all fifteen ensemble members (see Supplementary Material, Figure S20), and as expected, the future changes are slightly lower and more homogeneous due to the averaging across a larger ensemble, and the Historical range was far greater, especially over the mountainous regions.

Focusing on a highly non-homogeneous country, such as Norway, it is clear that the spatial differences in extreme winds are larger than the ensemble mean changes from one future time slice to the next (Fig. 6). While the future changes in extreme winds are small in almost all locations, these represent subtle changes to the upper tail of the distribution. An alternative approach to investigate the effects of such changes is to consider the changes in return frequencies of the extreme events. The bottom row of Fig. 6 shows the return frequency in years, of events with the same magnitude as the 30-year event in the Historical period. Lower values (i.e. <30) indicate that these events occur more frequently in the future. A few locations across Norway show consistently increasing or decreasing frequency in extreme winds, however, the picture is very heterogeneous.

The spatial differences in the magnitudes of extreme winds and the non-homogeneous changes in their frequencies both underscore the importance of local context when assessing extreme winds for adaptation planning at specific locations. However, the question remains, can we make some general statements about future changes of extreme winds across Europe projected by the Euro-CORDEX simulations?

In an attempt to answer this question, we divide the European domain into three distinct regions: a Northern region mainly covering Scandinavia and Scotland, a Central region covering Central Europe and the southern U.K., and a Southern region covering the Mediterranean (Fig. 7). These are separated at latitudes of 44°N and 55°N. Since the primary interest in studying extreme winds is the impact they have on society, we focus here on the extreme winds over land where the bulk of society's infrastructure is located, although extreme winds over sea also affect society. The frequencies of the extreme wind events over land are compared between the Historical period and the Near, Mid, and Far Future periods, with the median taken for each region across all 15 ensemble members (Fig. 7). For example, the median 70-year return level wind in the Historical period in the Northern region, is projected to have a return frequency of around 65 years in the Near future period, 58 years in the Mid future period, and around 50 years in the Far future period.

In all three regions, the frequency of return events consistently increase across the Near, Mid, and Far future periods. The change between the Historical and Near future periods is larger than between any of the other future periods in every region. This is likely a result of the changes arising from switching from Historical forcings to RCP8.5 forcings. The Southern region shows a much greater change in the frequency of future extreme wind events, with an Historical 100-year return event projected to occur with a frequency of around 58 years. While this approach does provide us with an overview of the general change in future extreme winds over Europe as projected by the models, it is important to remember the heterogeneous nature of extreme winds, especially when undertaking assessments for local-scale adaptation planning.

6. Discussion and conclusions

In this work we have examined the extreme winds in fifteen high-resolution (~12 km grid spacing) simulations where multiple RCMs have been used to downscale multiple GCMs. These RCM-GCM pairs form a subset of the much larger Euro-CORDEX ensemble and constitute what was available in 2018/19 when the study began. The extreme events in our Euro-CORDEX subset were assessed using a peaks-over-threshold approach with a GPD fitted to each grid point in each model. Return levels and frequencies were then analysed. The high horizontal resolution of the RCMs allows for realistic fine scale structure to be seen in the extreme winds across Europe and over the surrounding oceans and seas. The effects of individual mountain valleys, drag from cities, and even storm tracks over the seas are all visible, and all have a strong influence on the extreme winds on a local scale. Such details are absent

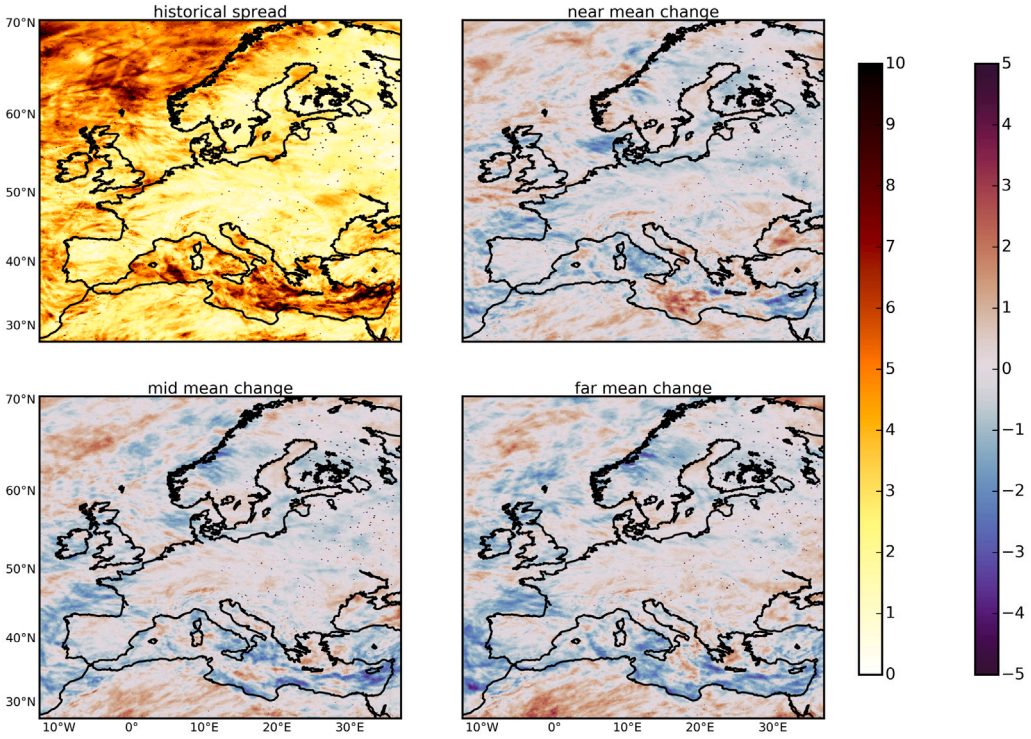

Fig. 5. Range of the 30-year return wind speed between the five SMHI simulations for our historical period (top left) and their mean change from our historical to our near future (top right), mid-future (bottom left), and far future (bottom right) periods. Units are ms^{-1}.

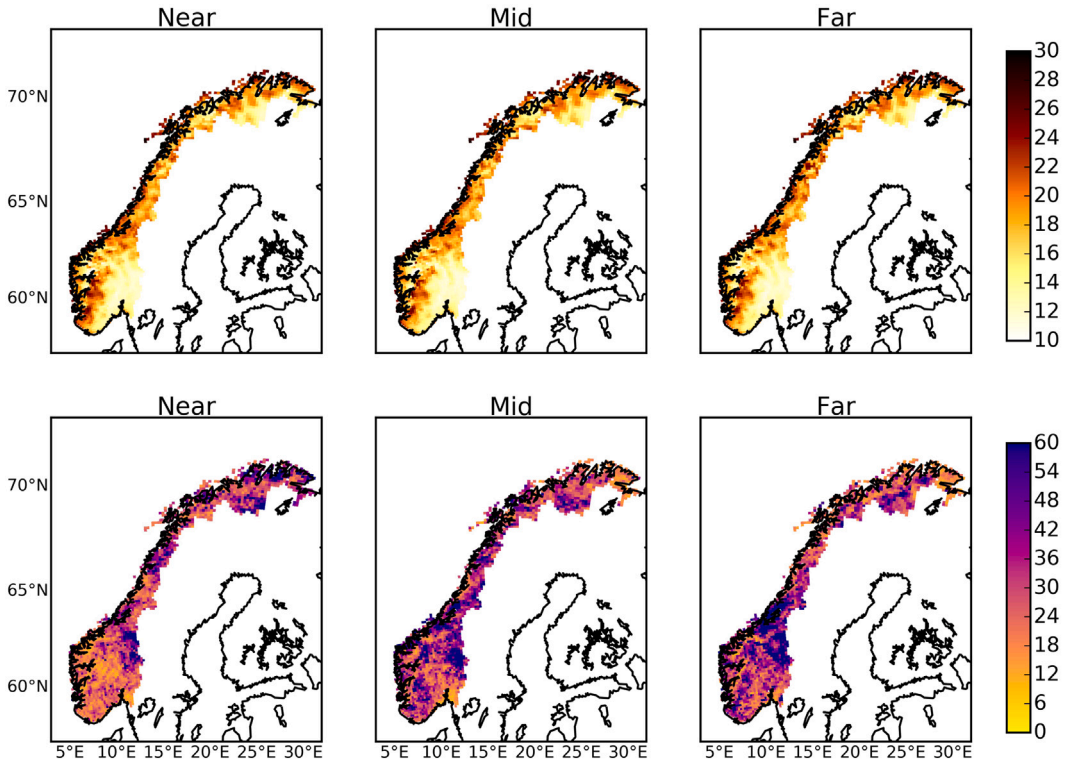

Fig. 6. Median of 30-year return wind speed (top row) and change in frequency of 30-year return event (bottom row) across all 15 ensemble members for our near (left), mid (middle), and far (right) future periods over Norway. Units are ms^{-1} for return wind speeds (top row) and years for frequency of return event (bottom row).

from previous dynamical downscaling efforts (e.g. ENSEMBLES, PRUDENCE) and are therefore missing from previous assessments (Donat et al., 2011; Pryor et al., 2012; Outten and Esau, 2013).

The value of the higher resolution was most readily apparent when compared to the 0.44°horizontal resolution simulations also produced under the Euro-CORDEX initiative (Fig. 4). These lower resolution

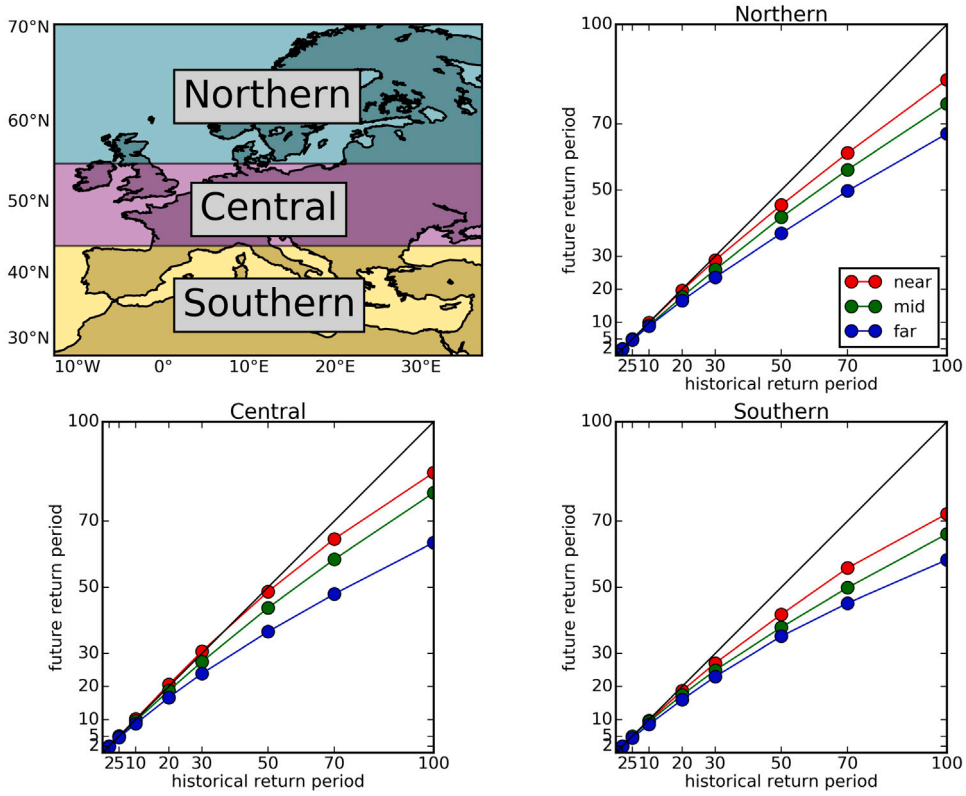

Fig. 7. European domain divided into a Northern, Central, and Southern region (top left). Change in return frequency of different levels of return event for our historical period compared to our near (red), mid (green), and far (blue) future period. The return frequencies are calculated as the median over land in the Northern (top right), Central (bottom left), and Southern (bottom right) regions. Unites are ms^{-1}. (For interpretation of the references to colour in this figure legend, the reader is referred to the web version of this article.)

simulations underestimated the structure and intensity of extreme winds in coastal and mountainous regions, both regions where extreme winds and their impacts are of critical importance. Perhaps more surprising was the complete lack of extreme winds over the inland seas in the coarse resolution simulations compared to their high resolution counterparts. This shortcoming was especially pronounced over the Mediterranean. Europe is unique in having such high resolution simulations under the CORDEX initiative, with most other CORDEX domains having only the standard 0.44°resolution. More recently the CORDEX-CORE simulations have aimed to cover all domains with a limited set of RCM-GCM pairs at 0.22°resolution (Remedio et al., 2019). This resolution puts CORDEX-CORE on par with ENSEMBLES simulations so, barring major advancements in the gust characterisations, it is unlikely that extreme winds will be well-represented. The deficiencies described here raise questions as to the value of the standard CORDEX resolution simulations for assessing extreme winds elsewhere in the world.

The fine scale structure highlights the heterogeneity of the extreme winds over land (Figs. 1–6). This underscores the need for assessments of extreme winds to be done on the local-scale, on a case-by-case basis. This is especially important when making assessments for adaptation planning and decision-making, when broad sweeping conclusions inferred from aggregated regional statistics could be misleading when applied to individual locations.

However, such aggregated statistics do have a place (e.g. IPCC reports, national assessments, regional assessments) and our analysis clearly shows the upscaled added value the high resolution ensemble provides (Fig. 4). In an attempt to make some overall assessment of projected changes in future extreme winds, the 21st Century simulations were divided into three time slices and the future change in the frequencies of extreme wind events were assessed. This was averaged over the fifteen high resolution ensemble members, and over land gridpoints for three regions of Europe; a Northern, Central, and Southern region. All three regions showed an increase in occurrence of extreme winds as we go further into the future (Fig. 7). For example, over the Northern region an extreme wind that has a return frequency of 100 years in the Historical period is projected to occur with a frequency of around 83 years in 2011–2040, 76 years in 2041–2070, and 67 years during 2071–2100.

While previous studies also found projected increases in extreme winds in RCMs over most of Europe, Donat et al. (2011) and Outten and Esau (2013) both found projected decreases of extreme winds over the Mediterranean. Our results suggest that the projections for extreme winds over the Southern region may increase as we go into the future. This is not an entirely fair comparison, however, as we have examined future extreme winds only over the land, thus excluding the Mediterranean Sea where the extreme winds are governed by the passage of stochastically occurring storms (however, including the sea does not substantively change our results). Whether the inconsistency arises due to differences in resolution, analytical approach, driving GCMs, or simply arises from sampling (see below) is not immediately clear.

There are a few caveats to findings presented here that suggest future research directions. The first is concerned with the assessment of uncertainty in high-resolution climate simulations. The uncertainties associated with the return wind estimates have only been calculated for the single location of Bergen. The uncertainties are computationally costly to calculate and while for any single grid point, this cost is small, for the complete Euro-CORDEX domain consisting of 174,688 grid points, this quickly becomes impractical without access to HPC and parallelised coding. However, just as the projected future changes are small compared to the inter-model spread, so too would we expect the uncertainties to be small compared to this spread, based on the estimates for the Bergen location and the previous work of Outten and Esau (2013). A second caveat is related to ensemble size. This

study made use of a subset of the Euro-CORDEX simulations. The Euro-CORDEX ensemble has experienced explosive growth in the past year and now stands at over 55 members for RCP8.5 and 22 members for RCP2.6 (see e.g. Coppola et al., 2021) and it is still growing. Therefore, expanding our analysis to include a larger ensemble will be important to test the robustness of the results, especially with respect to the increases projected over southern Europe. We note that the increases projected for Northern and Central Europe appear to be robust across data sets, scenarios and resolutions. While increasing ensemble size has some clear benefits it will also present additional challenges with respect to the assessment of uncertainty.

Despite the progress made in assessing extreme winds with RCMs, a number of outstanding issues remain. Some are well known and relate to the assessment of any extreme event in an RCM. The GPD is a distribution for assessing only the extremes and, like the GEV, the tail of the distribution is very sensitive. Subtle changes in the data result in subtle changes to the bulk of the distribution but much larger changes in the upper tail, shifting the derived return levels. There are no complete solutions to this problem, and it is a consequence of attempting to assess events that are, by definition, rare. Using the peaks-over-threshold approach instead of the block maxima greatly increases the number of extreme events included in the assessment, which helps to limit this sensitivity. Another issue is that RCMs are at the end of a long chain, each link with potential sources of uncertainty, including: socio-economic assumptions, projected emissions scenarios, carbon cycle response and concentration projections, global climate sensitivity estimates, and finally, global model errors and regional climate model errors (Jones, 2000). New uncertainties are potentially introduced into the final projections from the RCM with each stage of this chain (Foley, 2010). However, this is not always the case as RCMs have also been shown to systematically reduce GCM biases (Sørland et al., 2018). For a review of RCMs including their limitations and caveats, see for example, Rummukainen (2010).

By far the most critical outstanding problem is the lack of an accurate observational data set against which to validate the models. Since extreme winds are highly localised, even those stations that do record the maximum observed daily wind speed are only representative of a very small area around that station. This greatly limits the possibility for creating a gridded data-set covering a large area such as Europe. However, given the economic losses to extreme winds suffered by Europe every year (MunichRe, 2011; MunichRE, 2020), the challenging task of developing a gridded observational data-set of winds, and even extreme winds, is a challenge worth tackling.

CRediT authorship contribution statement

Stephen Outten: Conceptualization, Methodology, Software, Formal analysis, Visualisation, Writing – original draft. **Stefan Sobolowski:** Conceptualization, Securing funding, Visualisation, Writing – review and editing, Project administration.

Declaration of competing interest

The authors declare that they have no known competing financial interests or personal relationships that could have appeared to influence the work reported in this paper.

Acknowledgements

This publication was supported by the EMULATE project, funded through basic institutional support from Norwegian Department of Education to the Bjerknes Centre for Climate Research. The authors gratefully acknowledge all the participating modelling centres for their contributions to the Euro-CORDEX initiative and making their data available via the Earth System Grid Federation.

Appendix A. Supplementary data

Supplementary material related to this article can be found online at https://doi.org/10.1016/j.wace.2021.100363.

References

Balkema, A.A., de Hann, L., 1974. Residual lifetime at great age. Ann. Probab. 2, 792–804.

Beniston, M., 2004. The 2003 heat wave in Europe: a shape of things to come? Geophys. Res. Lett. 31, L02202. http://dx.doi.org/10.1029/2003GL018857.

Beniston, M., Stephenson, D.B., Christensen, O.B., Ferro, C.A.T., Frei, C., Goyette, S., Halsnaes, K., Holt, T., Jylha, K., Kofli, B., Palutikof, J., Scholl, R., Semmler, T., Woth, K., 2007. Future extreme events in European climate: an exploration of regional climate model projections. Clim. Change 81, 71–95.

Coles, S., 2001. An Introduction to Statistical Modelling of Extreme Values. Springer, London, 208 p.

Coppola, E., Nogherotto, R., Ciarlo', J.M., Giorgi, F., Meijgaard, E.v., Kadygrov, N., Iles, C., Corre, L., Sandstad, M., Somot, S., Nabat, P., Vautard, R., Levavasseur, G., Schwingshackl, C., Sillmann, J., Kjellström, E., Nikulin, G., Aalbers, E., Lenderink, G., Christensen, O.B., Boberg, F., Sørland, S.L., Demory, M.-E., Bülow, K., Teichmann, C., Warrach-Sagi, K., Wulfmeyer, V., 2021. Assessment of the European climate projections as simulated by the large EURO-CORDEX regional and global climate model ensemble. J. Geophys. Res.: Atmos. 126 (4), http://dx.doi.org/10.1029/2019JD032356, e2019JD032356. https://agupubs.onlinelibrary.wiley.com/doi/abs/10.1029/2019JD032356, _eprint: https://agupubs.onlinelibrary.wiley.com/doi/pdf/10.1029/2019JD032356.

Della-Marta, P.M., Mathis, H., Frei, C., Liniger, M., Kleinn, J., Appenzeller, C., 2009. The return period of wind storms over Europe. Int. J. Climatol. 29, 437–459.

Donat, M.G., Leckebusch, G.C., Wild, S., Ulbrich, U., 2011. Future changes in European winter storm losses and extreme wind speeds inferred from GCM and RCM multi-model simulations. Nat. Hazards Earth Syst. Sci. 11, 1351–1370. http://dx.doi.org/10.5194/nhess-11-1351-2011.

Donat, M.G., Renggli, D., Wild, S., Alexander, L.V., Leckebusch, G.C., Ulbrich, U., 2016. Reanalysis suggests long-term upward trends in European storminess since 1871. Geophys. Res. Lett. 38, L14703. http://dx.doi.org/10.1029/2011GL047995.

Fisher, R.A., Tippett, L.H.C., 1928. Limiting forms of the frequency distribution of the largest or smallest member of a sample. Math. Proc. Camb. Phil. Soc. 24, 180–190.

Foley, A.M., 2010. Uncertainty in regional climate modelling: A review. Prog. Phys. Geogr. Earth Environ. 34, 647–670. http://dx.doi.org/10.1177/0309133310375654.

Forzieri, G., Feyen, L., Russo, S., Vousdoukas, M., Alfieri, L., Outten, S., Migliavacca, M., Bianchi, A., Rojas, R., A., C., 2016. Multi-hazard assessment in Europe under climate change. Clim. Change 137, 105–119. http://dx.doi.org/10.1007/s10584-016-1661-x.

Giorgi, F., Gutowski, W.J., 2015. Regional dynamical downscaling and the CORDEX initiative. Annu. Rev. Environ. Resour. 40 (1), 467–490. http://dx.doi.org/10.1146/annurev-environ-102014-021217.

Grams, C.M., Binder, H., Pfahl, S., Piaget, N., Wernli, H., 2014. Atmospheric processes triggering the central European floods in June 2013. Nat. Hazards Earth Syst. Sci. 14, 1691–1702. http://dx.doi.org/10.5194/nhess-14-1691-2014.

Grumm, R.H., 2011. The central European and Russian heat event of July–August 2010. Bull. Am. Meteorol. Soc. 92, 1285–1296.

Gumbel, E.J., 1958. Statistics of Extremes. Columbia University Press, New York.

Hewson, T.D., Neu, U., 2015. Cyclones, windstorms and the IMILAST project. Tellus A 67, 27128. http://dx.doi.org/10.3402/tellusa.v67.27128.

Jacob, D., Teichmann, C., Sobolowski, S., Katragkou, E., Anders, I., Belda, M., Benestad, R., Boberg, F., Buonomo, E., Cardoso, R.M., Casanueva, A., Christensen, O.B., Christensen, J.H., Coppola, E., De Cruz, L., Davin, E.L., Dobler, A., Domínguez, M., Fealy, R., Fernandez, J., Gaertner, M.A., García-Díez, M., Giorgi, F., Gobiet, A., Goergen, K., Gómez-Navarro, J.J., Alemán, J.J.G., Gutiérrez, C., Gutiérrez, J.M., Güttler, I., Haensler, A., Halenka, T.s., Jerez, S., Jiménez-Guerrero, P., Jones, R.G., Keuler, K., Kjellström, E., Knist, S., Kotlarski, S., Maraun, D., van Meijgaard, E., Mercogliano, P., Montávez, J.P., Navarra, A., Nikulin, G., de Noblet-Ducoudré, N., Panitz, H.-J., Pfeifer, S., Piazza, M., Pichelli, E., Pietikäinen, J.-P., Prein, A.F., Preuschmann, S., Rechid, D., Rockel, B., Romera, R., Sánchez, E., Sieck, K., Soares, P.M.M., Somot, S., Srnec, L., Sørland, S.L., Termonia, P., Truhetz, H., Vautard, R., Warrach-Sagi, K., Wulfmeyer, V., 2020. Regional climate downscaling over Europe: perspectives from the EURO-CORDEX community. Reg. Environ. Change 20 (2), 51. http://dx.doi.org/10.1007/s10113-020-01606-9.

Jones, R.N., 2000. Managing uncertainty in climate change projections - issues for impact assessment - an editorial comment. Clim. Change 45, 403–419.

Koh, T., Djamil, Y.S., Teo, C., 2011. Statistical dynamics of tropical wind in radiosonde data. Atmos. Chem. Phys. 11, 4177–4189. http://dx.doi.org/10.5194/acp-11-4177-2011.

Kunz, M., Mohr, S., Rauthe, M., Lux, R., Kottmeier, C., 2010. Assessment of extreme wind speeds from regional climate models – part 1: Estimation of return values and their evaluation. Nat. Hazards Earth Syst. Sci. 10, 907–922. http://dx.doi.org/10.5194/nhess-10-907-2010.

Larsen, X.G., Mann, J., 2006. The effects of disjunct sampling and averaging time on maximum mean wind speeds. J. Wind Eng. Ind. Aerodyn. 94, 581–602.

Lun, I.Y.F., Lam, J.C., 2000. A study of Weibull parameters using long-term wind observations. Renew. Energy 20, 145–153.

MunichRe, 2011. Topics GEO, Natural Catastrophes 2011 Analyses Assessments Positions. Munich Reinsurance Company Publications, Munich, pp. 1–49.

MunichRE, 2020. Natural catastrophe statistics online – the NatCatSERVICE analysis tool. https://www.munichre.com/en/solutions/for-industry-clients/natcatservice.html.

Myhre, G., Shindell, D., Bréon, F.-M., Collins, W., Fuglestvedt, J., Huang, J., Koch, D., Lamarque, J.-F., Lee, D., Mendoza, B., Nakajima, T., Robock, A., Stephens, G., Takemura, T., Zhang, H., 2013. Climate change 2013: The physical science basis. In: Stocker, T.F., Qin, D., Plattner, G.K., Tignor, M., Allen, S.K., Boschung, J., Nauels, A., Xia, Y., Bex, V., Midgley, P.M. (Eds.), Contribution of Working Group I to the Fifth Assessment Report of the Intergovernmental Panel on Climate Change. Cambridge University Press, Cambridge, United Kingdom and New York, NY, USA, pp. 659–740. http://dx.doi.org/10.1017/CBO9781107415324.018.

Nikulin, G., Kjellstrom, E., Hansson, U., Strandberg, G., Ullerstig, A., 2011. Evaluation and future projections of temperature, precipitation and wind extremes over Europe in an ensemble of regional climate simulations. Tellus A 63, 41–55. http://dx.doi.org/10.1111/j.1600-0870.2010.00466.x.

Outten, S., Esau, I., 2013. Extreme winds over europe in the ENSEMBLES regional climate models. Atmos. Chem. Phys. 13, 1–10. http://dx.doi.org/10.5194/acp-13-1-2013.

Palutikof, J.P., Brabson, B.B., H., L.D., Adcock, S.T., 1999. A review of methods to calculate extreme wind speeds. Meteorol. Appl. 6, 119–132. http://dx.doi.org/10.1017/S1350482799001103.

Perrin, O., Rootzen, H., Taesler, R., 2006. A discussion of statisti- cal methods used to estimate extreme wind speeds. Theor. Appl. Climatol. 85, 203–215.

Pickands, J., 1975. Statistical inference using extreme order statistics. Ann. Statist. 3, 119–131.

Pryor, S.C., Barthelmie, R.J., Clausen, N.E., Drews, M., MacKellar, N., Kjellström, E., 2012. Analyses of possible changes in intense and extreme wind speeds over Northern Europe under climate change scenarios. Clim. Dynam. 38, 189–208.

Quine, C.P., 2013. Estimation of mean wind climate and probability of strong winds for wind risk assessment. Forestry 73, 247–258.

Remedio, A.R., Teichmann, C., Buntemeyer, L., Sieck, K., Weber, T., Rechid, D., Hoffmann, P., Nam, C., Kotova, L., Jacob, D., 2019. Evaluation of new CORDEX simulations using an updated Köppen–Trewartha climate classification. Atmosphere 10 (11), 726. http://dx.doi.org/10.3390/atmos10110726, https://www.mdpi.com/2073-4433/10/11/726.

Robine, J.M., Cheung, S.L.K., Sophie, L.R., Oyen, H.V., Griffiths, C., Michel, J.P., Hermann, F.R., 2008. Death toll exceeded 70,000 in Europe during the summer of 2003. Comptes Rend. Biol. 331, 171–178. http://dx.doi.org/10.1016/j.crvi.2007.12.001.

Rockel, B., Woth, K., 2007. Extremes of near-surface wind speed over Europe and their future changes as estimated from an ensemble of RCM simulations. Clim. Change 81, 267–280.

Rummukainen, M., 2010. State-of-the-art with regional climate models. Wiley Interdiscip. Rev. – Clim. Change 1, 82–96.

Scaife, A., Knight, J., 2008. Ensemble simulations of the cold European winter of 2005–2006. Q. J. R. Meteorol. Soc. 134, 1647–1659. http://dx.doi.org/10.1002/qj.312.

Schwierz, C., Kollner-Heck, P., Mutter, E., Bresch, D., Vidale, P., Wild, M., Schär, C., 2010. Modelling European winter wind storm losses in current and future climate. Clim. Change 101, 485–514.

Sørland, S.L., Schär, C., Lüthi, D., Kjellström, E., 2018. Bias patterns and climate change signals in GCM-RCM model chains. Environ. Res. Lett. 13 (7), 074017. http://dx.doi.org/10.1088/1748-9326/aacc77.

Ulbrich, U., Brücher, T., Fink, A.H., Leckebusch, G.C.K.A., Pinto, J.G., 2003. The central European floods of august 2002:Part 1 – rainfall periods and flood development. Weather 58.

Vautard, R., Kadygrov, N., Iles, C., Boberg, F., Buonomo, E., Bülow, K., Coppola, E., Corre, L., Meijgaard, E.v., Nogherotto, R., Sandstad, M., Schwingshackl, C., Somot, S., Aalbers, E., Christensen, O.B., Ciarlò, J.M., Demory, M.-E., Giorgi, F., Jacob, D., Jones, R.G., Keuler, K., Kjellström, E., Lenderink, G., Levavasseur, G., Nikulin, G., Sillmann, J., Solidoro, C., Sørland, S.L., Steger, C., Teichmann, C., Warrach-Sagi, K., Wulfmeyer, V., Evaluation of the large EURO-CORDEX regional climate model ensemble, J. Geophys. Res.: Atmos. n/a e2019JD032344, http://dx.doi.org/10.1029/2019JD032344, https://agupubs.onlinelibrary.wiley.com/doi/abs/10.1029/2019JD032344, _eprint: https://agupubs.onlinelibrary.wiley.com/doi/pdf/10.1029/2019JD032344.

van Vuuren, D., Edmonds, J., Kainuma, M., Riahi, K., Thomson, A., Hibbard, K., G.C., H., Kram, T., Krey, V., Lamarque, J.-F., Masui, T., Meinshausen, M., Nakicenovic, N., Smith, S., Rose, S., 2011. The representative concentration pathways: an overview. Clim. Change 109, http://dx.doi.org/10.1007/s10584-011-0148-z.

Van de Vyver, H., Delcloo, A.W., 2011. Stable estimations for ex- treme wind speeds. An application to Belgium. Theor. Appl. Climatol. 417–429. http://dx.doi.org/10.1007/s00704-010-0365-9.

Wang, X.L., Wan, H., Zwiers, F.W., Swail, V.R., Compo, G.P., Allan, R.J., Vose, R.S., Jourdain, S., Yin, X., 2011. Trends and low- frequency variability of storminess over western Europe 1878–2007. Clim. Dynam. 37, 2355–2371.